A Novel Frequency Reconfigurable Polarization Converter Based on Active Metasurface

Guangyao Liu, Jiaqi Han, Xiaohe Gao, Haixia Liu*, and Long Li**

Key Laboratory of High Speed Circuit Design and EMC of Ministry of Education
School of Electronic Engineering, Collaborative Innovation Center of Information Sensing and Understanding
Xidian University, Xi'an 710071, China
*hxliu@xidian.edu.cn, **lilong@mail.xidian.edu.cn

Abstract ─ In this paper, a novel frequency reconfigureable polarization converter (FRPC) based on active metasurface tuned by positive-intrinsic-negative (PIN) diodes is proposed. The metasurface unit cell of the FRPC consists of truncated metal square patches and bias lines, which are all etched on a substrate backed by a metal ground. On one hand, the FRPC can convert linearly polarized waves along the *x*- and *y*-axis into left- and right-hand circularly polarized waves from 5.13 to 5.61 GHz and from 5.37 to 6.72 GHz when all PIN diodes are turned ON and OFF, respectively. On the other hand, the proposed FRPC shows good angle stabilities when the incident angle ranges from 0° to 30° over the dual frequency bands. The simulated results show that the total 3 dB axial ratio relative bandwidth is more than 26%. To validate the polarization converter, a prototype of the FRPC is fabricated and measured. Measured results agree well with the simulation ones.

Index Terms ─ Active metasurface, frequency reconfigurable, PIN diode, polarization converter.

I. INTRODUCTION

Recently, due to the appearance of metasurface, manipulations of electromagnetic waves become more flexibly. Thereby, a series of progress has been achieved in the microwave, millimeter wave, terahertz and other frequency bands [1-8]. Applications include planar lenses, reflectarray and transmitarray antennas, digitally encoded antennas, etc. As the communication frequency bands become increasingly tight and the requirement of radar cross-section (RCS) reduction, multiple polarization methods are adopted to enhance the working band reuse capability. Some metasurface polarization converters (MPCs) have outstanding conversion efficiency [9,10]. And one or more polarization conversions mode can be implemented in a wide band or multiple bands [11]. At the same time, the thickness of the MPCs can be greatly reduced [12,13]. So the MPCs as a way to obtain multi-polarization have got growing research interest. So far, there have been many MPCs devices that implement transmissive or reflective linear-to-linear polarization, linear-to-circular polarization, and circular-to-circular polarization. For example, a bi-layered chiral metamaterial as a transmission polarization converter has been achieved, through which linear polarized (LP) waves can be converted into cross-polarization waves in a wideband [14]. Akbari et al. [15] proposed a broadband polarization converter operating at Ka band is realized by using a multi-layer board structure, and its 3 dB axial ratio (AR) relative bandwidth reaches 42%, meanwhile with an insertion loss less than 0.5 dB. References [16] demonstrated a novel THz half-wave polarization converter for cross-polarization conversions of both linear and circular polarizations. Furthermore, the polarizer can also be regulated by graphene. However, functionalities of the above MPCs cannot be changed after fabrication.

Then, the reconfigurable polarization converters (RPCs) based on metasurface have been reported. In [17], a polarization-reconfigurable converter using multi-layer frequency selective surface was proposed to convert the linear polarization (LP) into LP, right-hand circular polarization (RHCP) and left-hand circular polarization (LHCP) by mechanically rotating the metasurface screen. However, it is difficult to switch the device states quickly and exactly because of the mechanical rotation. In order to solve this shortcoming, some MPCs combined with active components (e.g., varactors, PIN diodes, MEMS) are proposed. Ratni et al. [18] loaded a varactor on each metasurface unit, and by adjusting the bias voltage load on the varactors, the RPC can convert LP into circular polarization (CP) in different frequency bands. But the performance of the 3 dB AR bandwidth is relative limited 10%. Apart from this, compared to the PIN diodes, varactors and MEMS show higher loss and their bias circuits are more complicated [19,20].

In this paper, a novel frequency reconfigurable polarization converter (FRPC) based on the reflective metasurface and PIN diodes is proposed. When the PIN diodes are turned ON and OFF, the FRPC can convert LP

Submitted On: December 28, 2018
Accepted On: May 6, 2019

waves into CP waves in successive different frequency bands. This paper is organized as follows. In Section II, the structure of FRPC is presented and operational principle of tuning the polarization state of an incident LP wave is described. Section III provides the experimental results and compares them with the simulated results. Finally, the paper is concluded in Section IV.

II. DESIGN AND ANALYSES

A. Structure of the FRPC unit

The unit of the proposed FRPC is illustrated in Fig. 1. The 3-D topology expanded view is shown in Fig. 1 (a), which consists of two metal layers, PIN diode, inductor and one dielectric layer. These two metal layers are composed of a metal ground on the back of the dielectric slab and a metasurface which is the truncated square patch with internally slotted. The bias line is deliberately designed to minimize the biasing circuit loss and simplify the structure. The biasing point is positioned at the zero-electric-field point along the non-radiating edge of the patch. Furthermore, in order to suppress the influence of the high frequency signal introduced by the power supply, a 27 nH inductor is placed between the bias line and the patch.

The top view and side view of the FRPC element is depicted in Fig. 1 (b). By optimization, the geometric parameters of the unit element are as follows: the patch with edge length W = 17 mm and is truncated a corner with edge P2 = 11 mm. A gap with width Gap = 0.45 mm is etched on the patch. And the gap is placed P1 = 4.2 mm from corner and parallels to the diagonal direction of the patch. In addition, the width of a bias line is Bia_*w* = 0.8 mm. The thickness and edge length of F4B substrate are H = 3.3 mm and *L* = 20 mm, which are about $\lambda_0/15$ and $\lambda_0/3$ respectively, where λ_0 is the wavelength at the center frequency. The diameter of the via from the top to the metal ground is Via_*r* = 0.6 mm.

MACOM MADP-000907-14020, which shows low insertion and can achieve an excellent electrical performance more than 10 GHz, is employed as the PIN diode in this paper [21]. For ON or OFF state, the PIN diode is modeled as a series of lumped resistance (R) and inductance (L) or capacitance (C) and inductance (L), respectively. Table 1 lists the homologous circuit parameters in the aimed frequency band.

B. Theory of operation

When the incident electromagnetic wave is LP wave with the electric field $\vec{E}_{in}$ in the *y*-direction and travels toward -*z*-direction. The incident electrical field radiated by an antenna can be written as two orthogonal linear components:

$$\vec{E}_{in} = \vec{E}_u + \vec{E}_v , \quad (1)$$

$$\left|\vec{E}_u\right| = \left|\vec{E}_v\right| , \quad (2)$$

where $\vec{E}_u$ and $\vec{E}_v$ are the components of the $\vec{E}_{in}$ in the *u* and *v* direction, respectively. $\left|\vec{E}_u\right|$ and $\left|\vec{E}_v\right|$ indicate the magnitude of the corresponding electric field.

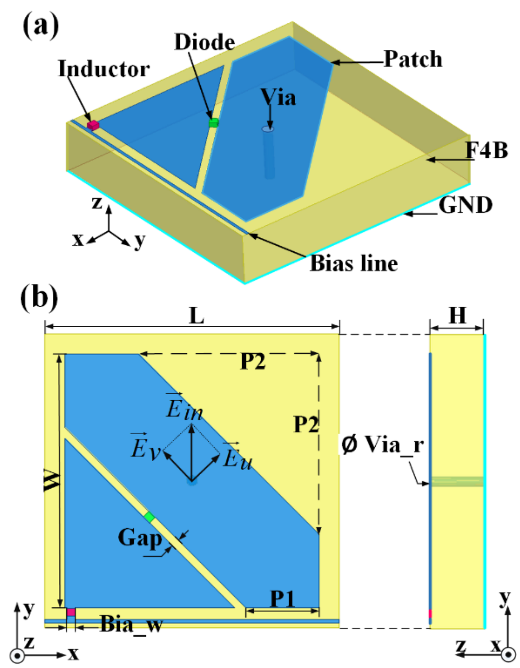

Fig. 1. Structure of the proposed FRPC unit cell: (a) 3-D topology expanded view, and (b) top view and side view.

Table 1: Equivalent circuit parameters of the PIN diode

Parameters	ON State	OFF State
R	7.8 Ω	-
L	30 pH	30 pH
C	-	0.025 pF

For the incident wave illuminates the FRPC element, the reflected electric field is also a sum of two orthogonal linearly polarized components:

$$\vec{E}_r = R(\vec{E}_u + \vec{E}_v) = R_u\vec{E}_u + R_v\vec{E}_v , \quad (3)$$

where R_u and R_v are the reflection coefficients for *u* direction and *v* direction. As R_u and R_v have the same magnitude $|R_u|$ and $|R_v|$. Meanwhile, the components of reflected electric field in two orthogonal linear directions with $\Delta\phi$ phase difference, which can be expressed as:

$$|R_u| = |R_v| , \quad (4)$$

$$\Delta\phi = \phi_u - \phi_v , \quad (5)$$

where ϕ_u and ϕ_v are the phase of $R_u\vec{E}_u$ and $R_v\vec{E}_v$, respectively. And if $\Delta\phi = \pm 90^\circ$ and $|R_u| = |R_v|$, the LP incident wave can be converted into the CP wave for transmitting in the free space. In this paper, according to the formula (4) and (5), we can get the following conclusions. When the incident LP wave is in *x*-direction with $\Delta\phi = 90^\circ$ phase difference, the incident wave can be converted to LHCP wave. In addition, since the metasurface unit structure is symmetric about the diagonal, as the incident wave is *y*-polarized with $\Delta\phi = -90^\circ$ phase difference, the LP wave can be converted to RHCP wave. For the sake of understanding the working mechanism of the FRPC well, the relation between the polarization of incident wave and the reflected wave from the FRPC array is depicted in Fig. 2.

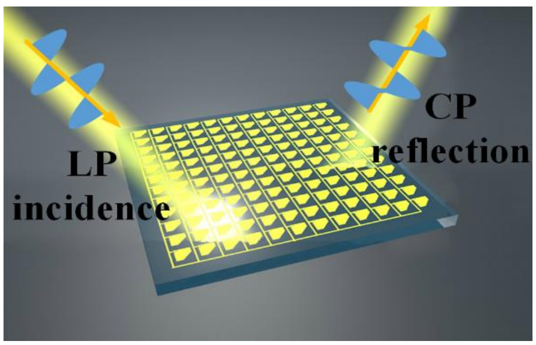

Fig. 2. Schematic model of a reflective polarization converter.

C. Simulation results

To verify the design functionality and explore the reflection characteristics, HFSS 15.0 is used to analyze and optimize the proposed element. The element is simulated by periodic boundary condition combined with Floquet port. Moreover, the PIN diode and inductor embedded on the unit cell are replaced by lumped elements in the corresponding cases under different operating states which are described above. As shown in Fig. 3 (a), the AR of the reflected wave varies with frequency when the incident wave is *x*-polarized or *y*-polarized, and the incident angle θ is to be zero in Floquet port. It is clear that the incident wave polarization direction does not affect the polarization conversion performance of the FRPC. As PIN diode under different states, the 3 dB AR bandwidth and the corresponding center frequency are different, specific parameter indicators are listed in Table 2. It is worth mentioning that the 3 dB AR bandwidth in two states is continuous, so the polarization converter can achieve the 3dB AR relative bandwidth of 26.74%.

When the incident wave is *y*-polarized, the amplitude and phase difference of the reflected wave electric field in the *u* and *v* directions are plotted, as shown in Fig. 3 (b). In different operating frequency bands, the electric field amplitudes in both directions are almost equal, and the phase difference approximate to $\Delta\phi = -90^\circ$. Since the amplitudes of the incident electric fields in both directions are equal, according to formula (3), $|R_u|$ and $|R_v|$ are approximately equal. In order to clearly display the polarization states of the reflected wave, the current distributions on the patch are plotted at the center frequency of the two operating states, as shown in Figs. 4 (a) and (b). The surface current vector distributions ranges from 0° to 270° with a 90° interval. As the incident wave is in the y-polarized, the reflected wave is the RHCP wave in both states.

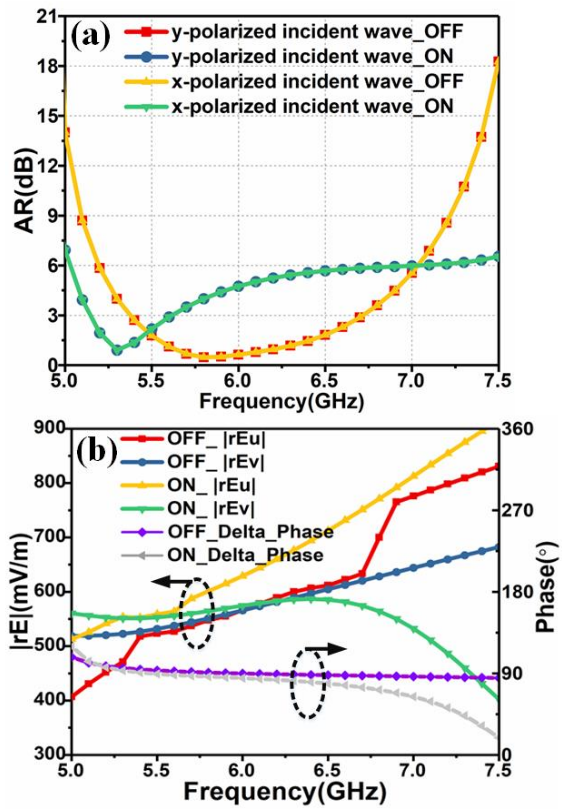

Fig. 3. Simulated reflected waves characteristics: (a) AR of the reflected wave varies with frequency when the incident wave is *x*-polarized or *y*-polarized, and (b) the amplitude and phase difference of the reflected electric field in the *u* and *v* directions.

Table 2: Index of reflected wave under different states

State	3dB AR Bandwidth (GHz)	Fractional Bandwidth	Center Frequency (GHz)
OFF	5.37 – 6.72	22.17%	6.05
ON	5.13 – 5.61	8.86%	5.37

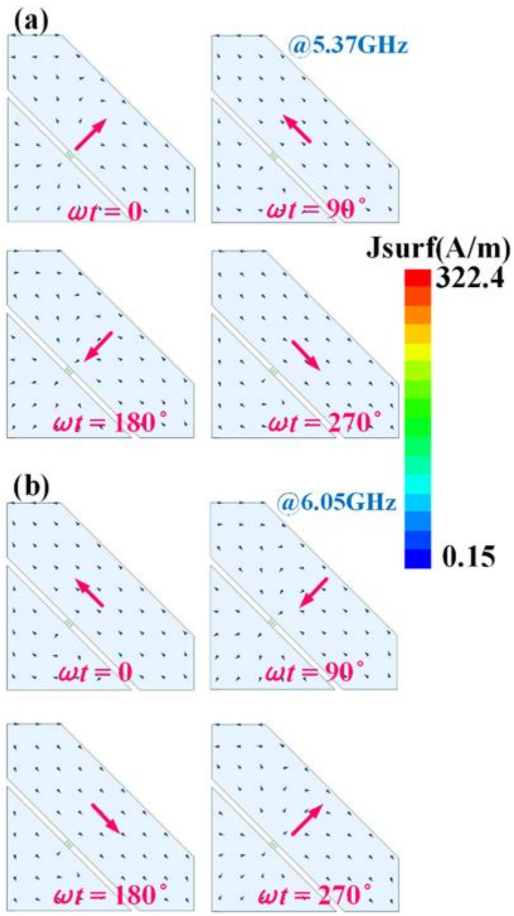

Fig. 4. Surface current distributions on the truncated square patch for four different instants: (a) RHCP at 5.37 GHz, and (b) RHCP at 6.05 GHz.

In addition, Fig. 5 (a) and 5 (b) illustrate the simulated AR characteristics for *y*-polarized electromagnetic waves with different incident angles θ under different states. It can be seen that the 3 dB AR relative bandwidth is more than 26%, when the incident angles range from 0° to 30°. In summary, although the waveforms are slightly different, the FRPC can efficiently reflect LP waves into CP waves in the conversion mode.

III. FABRICATION AND MEASUREMENT

In order to verify the simulation results, an FRPC metasurface array consisting of 18 × 18 unit cells is fabricated. The prototype with the size of 435 × 415 mm^2 is shown in Fig. 6, and all the bias lines are connected together and directed to the back of the array through a metallized via. In the measurements, two standard gain rectangular horn antennas are connected to an Agilent vector network analyzer E8364A as transmitter and receiver that are set on the front of the prototype. Besides, the bias voltage of the entire circuit is set to 5 volts. In operation, the transmitter horn antenna radiates *y*-polarized incident wave onto the prototype and the receiver horn antenna is used to receive *x*- and *y*-polarized reflected waves, respectively.

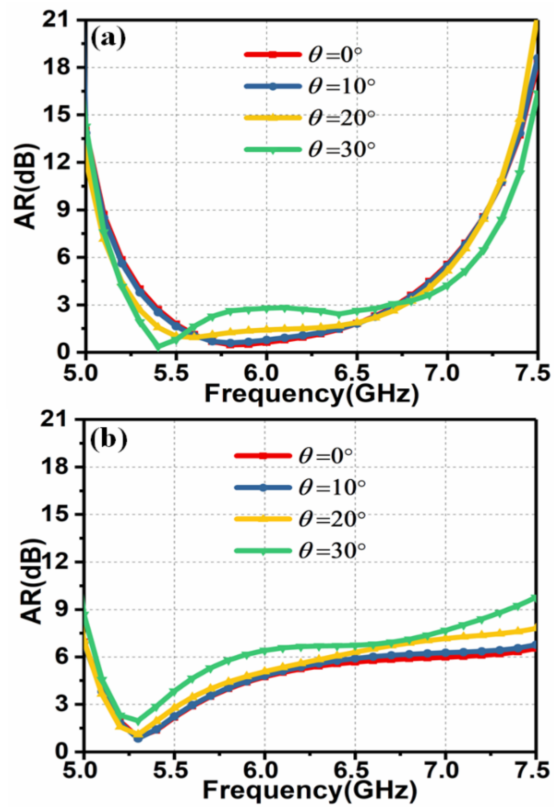

Fig. 5. Simulated AR characteristics for different incident angles at (a) OFF state and (b) ON state.

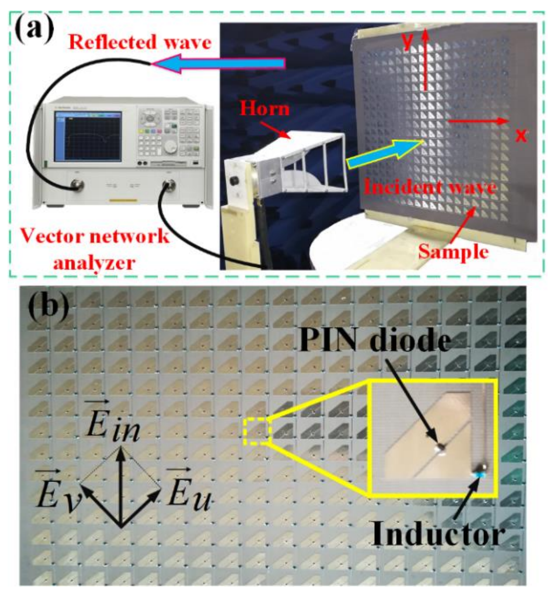

Fig. 6. 1-bit 18 × 18 FRPC prototype and measurement system: (a) system assembly and (b) sample zoom view.

The measured and simulated AR are illustrated in Fig. 7, there is a high consistency between the measured results and simulated results except a little error. In measurements, 3dB AR relative bandwidth of the FRPC is 8.23% (5.24–5.69 GHz) when the diodes are turned on, and the corresponding value is 21.12% (5.42–6.7 GHz) when the diodes are turned off. This difference with simulation results may be caused by tolerances in the fabrication and measurement processes. Thus, the measured results conform to the operating frequency band of the FRPC can be reconfigured by adjusting the state of the PIN diodes.

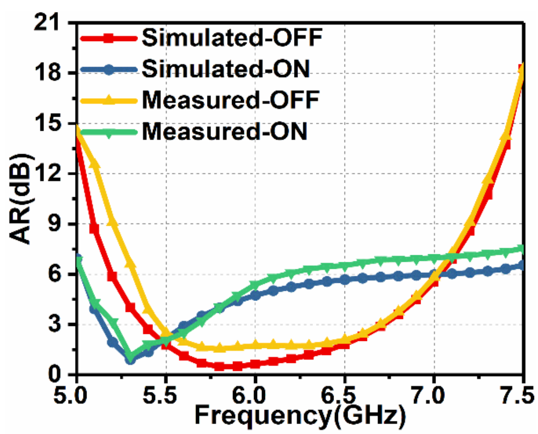

Fig. 7. Measured and simulated AR for different states of PIN diode.

IV. CONCLUSION

In this paper, a novel FRPC is realized based on active metasurface, which can reconfigure the operating frequency by switching the states of the PIN diodes. An electronically tuned FRPC with 18 × 18 unit cells is thoroughly investigated with measurements. Both simulations and experimental results reveal that the proposed FRPC can convert the LP waves into LHCP (RHCP) waves from 5.13 to 5.61 GHz when the PIN diodes are turned ON. Moreover, the FRPC can convert the LP waves into LHCP (RHCP) waves from 5.37 to 6.72 GHz as the PIN diodes are turned OFF. In addition, the experimental results demonstrate that two states the FRPC can change the LP incident waves into CP reflected waves with the 3 dB AR relative bandwidths more than 24%. The FRPC has great potentials in RCS reduction, communication, and the CP reflectarray applications, etc.

ACKNOWLEDGMENT

This work is supported by Shaanxi Outstanding Youth Science Foundation (2019JC-15) and National Key R&D Program of China.

REFERENCES

[1] V. K. Kothapudi, et al., “A 6-Port two-dimensional 3×3 series-fed planar array antenna for dual-polarized X-band airborne synthetic. Aperture radar applications,” *IEEE Access*, vol. 6, pp. 12001-12007, Mar. 2018.

[2] Y. Dong, “Metamaterial-based antennas,” *Proceedings of the IEEE*, vol. 100, no. 7, pp. 2271-2285, July 2012.

[3] S. Yu, H. Liu, and Long Li, “Design of near-field focused metasurface for high efficient wireless power transfer with multi-focus characteristics,” *IEEE Transactions on Industrial Electronics*, vol. 66, no. 5, pp. 3993-4002, 2019.

[4] Y. Zhao, M. A. Belkin, and A. Alù, “Twisted optical metamaterials for planarized ultrathin broadband circular polarizers,” *Nature Communications*, vol. 3, 10.1038/ncomms1877, May 2012.

[5] A. A. High, et al., “Visible-frequency hyperbolic metasurface,” *Nature*, vol. 522, pp. 192-196, June 2015.

[6] N. Yu and F. Capasso, “Flat optics with designer metasurfaces,” *Nature Materials*, vol. 13, pp. 139-150, Jan. 2014.

[7] J. N. Gollub, et al., “Large metasurface aperture for millimeter wave computational imaging at the human-scale,” *Scientific Reports*, vol. 7, 10.1038/srep42650, Feb. 2017.

[8] C. L. Holloway, et al., “An overview of the theory and applications of metasurfaces: The two-dimensional equivalents of metamaterials,” *IEEE Antennas and Propagation Magazine*, vol. 54, no. 2, pp. 10-35, July 2012.

[9] H. L. Zhu, et al., “Linear-to-circular polarization conversion using metasurface,” *IEEE Transactions on Antennas and Propagation*, vol. 61, no. 9, pp. 4615-4623, Sept. 2013.

[10] Xi Gao, et al., “Ultrawideband and high-efficiency linear polarization converter based on double V-shaped metasurface” *IEEE Transactions on Antennas and Propagation*, vol. 63, no. 8, pp. 3522-3530, Aug. 2015.

[11] R. Li, et al., “High-efficiency cross polarization converters by plasmonic metasurface,” *Plasmonics*, vol. 10, no. 5, pp. 1167-1172, Oct. 2015.

[12] X. Liu, et al., “Three-band polarization converter based on reflective metasurface,” *IEEE Antennas and Wireless Propagation Letters*, vol. 16, pp. 924-927, Sep. 2016.

[13] Z. Li, et al., “Realizing broadband and invertible linear-to-circular polarization converter with ultra-thin single-layer metasurface,” *Scientific Reports*, vol. 5, 10.1038/srep18106, Dec. 2015.

[14] W. Mo, et al., “Ultrathin flexible terahertz

polarization converter based on metasurfaces," *Optics Express*, vol. 24, no. 12, pp. 13621-13627, June 2016.

[15] F. Mirzamohammadia, et al., "A bi-layered chiral metamaterial with high-performance broadband asymmetric transmission of linearly polarized wave," *International Journal of Electronics and Communications*, vol. 98, pp. 58-67, Jan. 2019.

[16] M. Akbari, et al., "Ka-band linear to circular polarization converter based on multilayer slab with broadband performance," *IEEE Access*, vol. 5, pp. 17927-17937, Aug. 2017.

[17] L. Peng, et al., "A novel THz half-wave polarization converter for cross-polarization conversions of both linear and circular polarizations and polarization conversion ratio regulating by graphene," *Journal of Lightwave Technology*, vol. 36, pp. 4250-4258, May 2018.

[18] L. Li, et al., "Novel polarization reconfigurable converter based on multilayer frequency-selective surfaces," *Proceedings of the IEEE*, vol. 103, no. 7, pp. 1057-1070, July 2015.

[19] B. Ratni, et al., "Electronic control of linear-to-circular polarization conversion using a reconfigurable metasurface," *Applied Physics Letters*, vol. 111, no. 21, 101063, Nov. 2017.

[20] B. Schoenlinner, et al., "Switchable low-loss RF MEMS Ka-band frequency-selective surface," *IEEE Transactions on Microwave Theory and Techniques*, vol. 52, no. 11, pp. 2474-2481, Nov. 2004.

[21] Mouser Electronics. Skyworks Solutions, Inc. SMP1340-040LF PIN Diode Data.

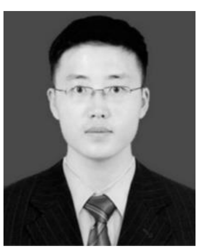

Guangyao Liu received the B.S. degrees in School of Electrical Engineering and Automation from Shanxi Agricultural University, in 2017. He is currently pursuing the M.S. degree with Xidian University, Xi'an, China. His research interests include reconfigurable metasurface and its applications.

Jiaqi Han received the B.S. degrees in School of Electrical and Electronics Engineering from Henan Normal University, Xinxiang, China, in 2014. He is currently pursuing the Ph.D. degree with Xidian University, Xi'an, China. His research interests include reconfigurable metasurface and its application.

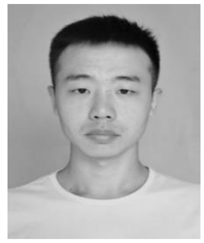

Xiaohe Gao received the B.Eng. degree in Electronic Information Engineering from North China Institute of Aerospace Engineering, Langfang China, in 2018. He is currently pursuing the Master of Engineering degree in Environmental Science and Engineering at Xidian University, Xian, China. His current research interests include the structural design of novel metamaterials and their applications in electromagnetic wave.

Haixia Liu (M'13) received the B.S. degree and the M.S. degree in Test and Measurement Technique and Instrumentation from Xidian University, Xi'an, China, in 1998 and 2001, respectively. She studied at Shizuoka University, Shizuoka, Japan, as a cooperative graduate in 2001. From 2002, she worked at Xidian University. She received the Ph.D. degrees in Electromagnetic Fields and Microwave Technology from Xidian University, Xi'an, China, in 2014. Her research interests include circuit analysis, frequency measurement and control, wireless power transfer, antennas, and electromagnetic compatibility.

Long Li (M'06-SM'11) received the B.E. and Ph.D. degrees in Electromagnetic Fields and Microwave Technology from Xidian University, Xi'an, China, in 1998 and 2005, respectively.

He was a Senior Research Associate in the Wireless Communications Research Center, City University of Hong Kong in 2006. He received the Japan Society for Promotion of Science (JSPS) Postdoctoral Fellowship and visited Tohoku University, Sendai, Japan, as a JSPS Fellow from Nov. 2006 to Nov. 2008. He was a Senior Visiting Scholar in the Pennsylvania State University, USA, from Dec. 2013 to July 2014. He is currently a Professor in the School of Electronic Engineering, Xidian University. He is also the Director of Key Lab of High Speed Circuit Design and EMC, Ministry of Education, China. His research interests include metamaterials, computational electromagnetics, electromagnetic compatibility, novel antennas, and wireless power transfer and harvesting technology.